Influence of Confinement on the Solvation and Rotational Dynamics of Coumarin 153 in Ethanol

Robert Baumann, Camilla Ferrante, Erwin Kneuper, Fred-Walter Deeg, and Christoph Bräuchle*

Department Chemie, Bereich Physikalische Chemie, Ludwig-Maximilians-Universität, Butenandtstrasse 5-13, D-81377 München, Germany

Received: October 9, 2002

The solvation and rotational dynamics of the chromophore coumarin 153 in ethanol confined in sol−gel glasses with average pore sizes of 50 and 25 Å have been investigated and compared with the dynamics of the respective bulk solution. The measurements show that no adsorption of the chromophore at the inner pore surface occurs. Nevertheless, the amplitude and the dynamics of the Stokes shift as well as the time-resolved anisotropy are drastically changed upon confinement. The solvation dynamics in the confined solutions show nonexponential behavior comparable to that in the bulk. However, the whole solvation process slows down, and the single decay-time constants characterizing it increase with decreasing pore size of the sol−gel glass. However, an increase of the mean rotational diffusion time constant sets in until the pore diameter decreases to less than 50 Å. Two phenomenological models are put forward to rationalize this behavior. The model of a surface solvent layer with changed physical properties such as the viscosity and dielectric constant focuses on the interaction of the liquid with the inner pore surface reducing the molecular mobility and resulting in longer relaxation times. The modified polarization field model takes into account the confinement and predicts a variation of the solvent's reaction field induced by a preferential alignment along the pore walls. Probably both effects are of relevance in the confined solutions investigated. Confinement affects the steady-state spectra and leads to a red shift of the absorption and a blue shift of the fluorescence.

1. Introduction

The important role of liquids in science, technology, and daily life has motivated a large number of investigations on structural, thermodynamic, and dynamic properties of liquid media. On the basis of the macroscopic hydrodynamic properties of liquids[1−6] and primarily dielectric measurements,[7−9] models to describe the molecular and collective motions have been developed[10−16] and successively improved.[17−27]

The detailed investigation of molecular processes in solutions is of particular interest to the chemist because the dynamics of the energy stabilization of solutes in liquids (i.e., solvation dynamics) is of vital importance to chemical reactions in liquid media.[28] The solvent can influence both the reaction path and the energetic states of the reactants and reaction products. Throughout the chemical reaction, the surrounding solvent molecules respond by reorganization and are able to dissipate the reaction energy that is set free. The nature of the solute−solvent interactions and the characteristic correlation lengths for these interactions are fundamental to this reorganization process.

By confining liquids within nanosized geometrical restraints, many of their physical and chemical properties change drastically.[29−32] Both the reduced volume of the interacting liquid and the forces between the confining surface and the liquid molecules influence the dynamics of these systems.

In natural systems, chemical reactions and transport processes often take place in microscopically small "solvent pools" such as cells, membranes, proteins, or micelles. And the relevance of confinement in technical fields such as catalysis, oil recovery, or medical industries has encouraged several research groups to simulate such small liquid cages and investigate the solvent properties with a restricted number of molecules. A large amount of experimental work has been done in the past decade to characterize the dynamics of confined liquids. The main focus in these investigations has been on rotational diffusion[33−47] and solvation dynamics[48−60] employing different techniques such as NMR,[35,61−64] Rayleigh wing spectroscopy,[37] Raman spectroscopy,[34,42] optical Kerr effect (OKE) spectroscopy,[36,38−40,43−46] and time-resolved luminescence.[41,42,48,50−59,65] But there are also reports of vibrational dephasing,[34] fluorescence lifetimes,[66] electronic energy transfer,[67] charge-transfer reactions,[54] and photoisomerizations[55] in confined systems. Our own group has used the OKE technique to study the influence of confinement on the behavior of complex molecular liquids that form ordered phases.[36,46] For the nematogenic liquid pentylcyanobiphenyl at temperatures far above the nematic−isotropic phase transition, the results are interpreted in terms of a two-phase model.[47]

Besides investigations of rotational diffusion, the study of solvation processes has been the second focus of experimental work on the dynamics of confined liquids. Solvation dynamics has been systematically studied in a large number of bulk liquids of different polarity[68−72] or polarizability.[71−73] In general, multiexponential behavior has been observed, which is interpreted in terms of a global process and compared with experimental data of the frequency-dependent dielectric constants of the pure liquids.

The theoretical treatment ranges from simple continuum theories,[15,16,18,74−76] which consider the solvent to be a pure hydrodynamic continuum, to more complex models,[21,22,24,25,77−80]

* Corresponding author. E-mail: Christoph.Braeuchle@cup.uni-muenchen.de.

10.1021/jp027172y CCC: $25.00
Published on Web 03/14/2003

where the molecular structure of the solvent is considered. The latter theories allow one to define the process of solvation in terms of solvation shells and especially to define the extensions and behavior of the first solvation shells around the solute. Molecular dynamics simulations[27,81,82] for simpler solvents are also available for comparison with the experimental findings.

To our knowledge, the first time-resolved investigation of solvation in confinement was published by Vajda et al.[53] in 1995. They investigated coumarin chromophores in a γ-cyclodextrin cavity dissolved in water. Their main observation was the appearance of new slow relaxation components in the restrictive geometry compared to bulk water. As possible candidates causing these additional components, they cite the motion of the probe molecule itself, the fluctuations of the γ-cyclodextrin ring, and the reorientation of highly constrained water molecules. Later, Das et al.[52] measured the solvation of coumarin 480 in a (solvent-free) zeolite cage. They found a very slow 8-ns solvation response that they associate with the motion of the probe molecule itself and the dynamics of the sodium ions in the cage.

The γ-cyclodextrin cavity and the zeolite cage represent voids with well-defined extensions and form, yet it is impossible to vary the size of the confining space in these samples. To investigate the interaction length scales in liquids and characterize the effects of confinement quantitatively, one needs a medium in which the size of the restrictive geometry can be systematically varied. In this respect, two kinds of materials seem to be especially suitable—micelles and porous sol−gel glasses—and solvation dynamics investigations in recent years have concentrated on these samples.

Lundgren et al.[48] were the first to use micelles, and they have shown that the solvation of a human serum albumine chromophore in water-filled aerosol-OT(AOT) reverse micelles takes place on a nanosecond time scale. Bhattacharyya's[54−56] group has performed time-resolved luminescence studies in a number of chromophore/water/reverse micelle samples. In contrast to the drastic slowing of the solvation dynamics in confined water (by 3 orders of magnitude), the time constants of processes such as intramolecular charge transfer[54] or photoisomerization[55] increase by only a factor of 3 to 4. They also performed solvation dynamics experiments with coumarin 480 in a sol−gel matrix at room temperature.[124] In their work, the dye is directly added to the aqueous solution from which the sol−gel glass is formed. The solvation dynamics is markedly slowed upon solidification of the gel. A direct comparison with the present work cannot be made since in it the dye solution was left to diffuse in the dry sol−gel glass and therefore can be solvated only inside the pores, whereas in their case the dye can also be trapped inside the sol−gel inorganic matrix.

More recently, Levinger 's group has performed solvation dynamics studies in reverse micelles while systematically varying the diameter of the micelle.[57,58] This group also investigated solvation dynamics in formamide-filled reverse micelles.[59] Whereas their vibrational investigations point to a liquid structure comparable to that of the bulk, the dynamics shows complete immobilization of the formamide in small micelles, which is similar to their data for water. They conclude that steady-state measurements are not always a good indicator of molecules in heterogeneous environments, and dynamics studies can provide information that is not otherwise obtainable.

Besides micelles, porous sol−gel glasses are the second class of materials that allow a simple variation of the dimensions of the confining space. Richert and co-workers have used these porous glasses extensively to study the behavior of supercooled liquids and the effect of geometric confinement on the glass transition. Whereas in their earlier investigations they relied on dielectric spectroscopy,[83−85] in more recent experiments they have also used time-resolved phosphorescence to characterize solvation dynamics in these very viscous confined liquids.[49,50] They interpret their results in terms of a surface layer with strongly frustrated dynamics whose thickness increases drastically upon the approach of the glass-transition temperature. We are using the same kind of porous sol−gel glasses in our investigations, but our work is focusing on solvation in mobile liquids far above the glass transition.

Whereas there is an abundance of theoretical work on solvation in polar liquids (see above), theory is lagging behind experiment in the area of confined liquids. Nandi and Bagchi[86] have analyzed the coumarin/cyclodextrin sample investigated by Vajda et al.[53] with a multishell continuum model and a molecular hydrodynamic theory. They find good agreement between experimental data and the molecular theory associating the drastic slowing down of the solvation response with the immobilization of the water molecules within the cyclodextrin cavity. An investigation by the same authors[87] suggests the existence of a shell of "biological" water around the proteins and the exchange of bound and free water within this shell are responsible for the bimodal behavior of water in biological systems. Recent papers by Senapati and Chandra[88,89] study dipolar liquids confined between two flat solid surfaces and in spherical cavities with molecular dynamics simulation techniques. They find that solvation is slowed at the interface compared to that in the bulk. However, they also point out the possible influence of surface roughness on dynamics close to the surface.

In recent experiments, we have measured the solvation and reorientational dynamics of nile blue in ethanol confined to porous sol−gel glasses[90] using the fluorescence upconversion method. These investigations on mostly adsorbed chromophores revealed an increase of the characteristic solvation dynamics decay times with decreasing pore size. The rotational diffusion of unadsorbed nile blue molecules in larger pores (75 Å) is identical to that of the bulk solution, whereas in the smaller pores (50 Å) the rotational diffusion is slowed.

To characterize the solvation process in these systems further, we have performed solvation dynamics and time-resolved anisotropy measurements on a different nonionic chromophore. Coumarin 153 was chosen because of its large fluorescence Stokes shift and the considerable amount of solvation dynamics data already available for this probe molecule.[17,18,91−96] In this paper, we will present experimental data on the solvation dynamics behavior of coumarin 153/ethanol solution confined in porous sol−gel glasses at room temperature obtained by means of the fluorescence upconversion technique.

The experimental setup and results are presented in sections 2 and 3, respectively. These results are discussed in section 3 in terms of two phenomenological models: the modified polarization-field model and the surface solvent-layer model. They both can explain the influence of the confinement and surface effects on solvation and rotational dynamics in restricted geometry resulting in a decrease of the characteristic time constants.

2. Experimental Section

A. Sample Preparation. The porous sol−gel glass samples were obtained from Geltech Inc. with a cylindrical shape of 5-mm diameter and 2.3-mm thickness. The samples investigated have average pore diameters of 25 and 50 Å and porosities of

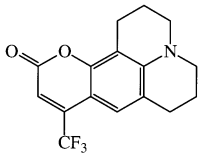

Figure 1. Structure of the chromophore coumarin 153.

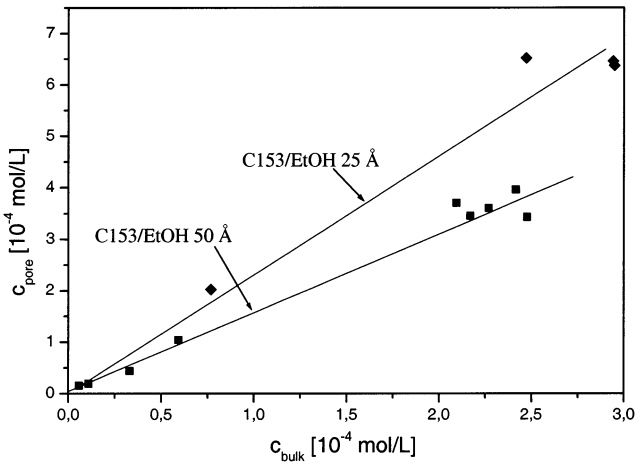

Figure 2. Inclusion isotherm of C153 in ethanol confined in sol−gel glasses 50 (◆) and 25 Å (■) in diameter.

47 and 61%, respectively. They were purified and modified as follows. To remove adsorbed water and other contaminations from the inner surface, the sol−gel was heated to 450 °C by a slow-temperature ramp and kept at that temperature for 1 day. To reduce the polarity of the inner pore surfaces, the polar OH groups were substituted by less polar $OSi(CH_3)OC_2H_5$ groups. To this end, the clean and dry sol−gel glass was immersed in a mixture of toluene and dichlordimethylsilane under a dry argon atmosphere to prevent water pollution of the sample. After 2 weeks, dry ethanol was added to the mixture to remove the chlorine residues. Then the sample was washed with toluene and cleaned with ethanol. After the evaporation of the solvent, the modified sol−gel glass was ready to be filled with the dye solution.

The chromophore coumarin 153 (C153) (Figure 1) was purchased from Radiant Dyes and used without any further purification. Highly purified ethanol (+99.99%, SeccoSolv) was obtained from Merck and used as received. For all measurements, solutions at low chromophore concentration ($<10^{-4}$ M) were prepared under a dry argon atmosphere to avoid water contamination of the sample.

The modified sol−gel glasses were filled with the solution by immersing them in a prepared bulk dye solution: equilibrium between the solution in the sol−gel samples and the bulk solution surrounding the glass is reached within 1 week. Synchronous absorption measurements of the solution in the sol−gel glass and in the solution surrounding the sample ensure the achievement of the equilibrium. By repeating this procedure with various starting concentrations in the bulk solution, inclusion isotherms (Figure 2) of the concentration ratio inside and outside the sol−gel glass can be established for different pore sizes. The filled samples were put into quartz cuvettes (Hellma) having a matching internal width of about 2.5 mm so that there is a negligible amount of solvent between the cuvette window and the sample surface.

B. Absorption and Fluorescence Spectra. To characterize the bulk dye solution as well as the confined systems, absorption and fluorescence spectra were taken. Absorption spectra were recorded with an Uvikon 860 spectrometer from Kontron Instruments providing a resolution of 1.0 nm. Fluorescence spectra were taken with a homebuilt spectrometer in which the sample was excited by the light of a helium−cadmium laser (Liconix) at 445 nm. The fluorescence was then detected by a Spex 1402 double monochromator and a Hamamatsu C31034 GaAs photomultiplier in combination with a single-photon counter (Stanford Research SR400). The spectra were recorded by a suitable computer program controlling the monochromator and reading the data from the single-photon counter.

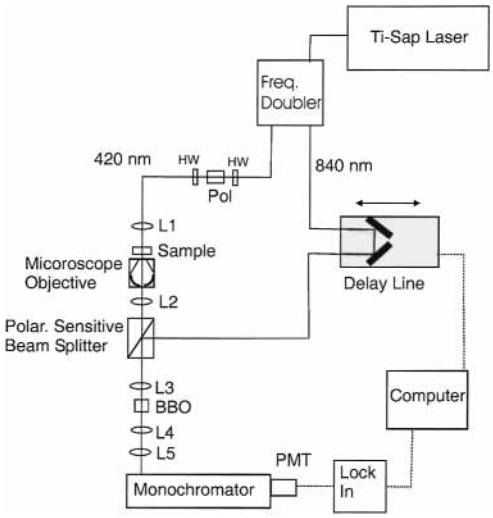

Figure 3. Experimental setup for fluorescence upconversion measurements.

C. Fluorescence Upconversion Spectroscopy. Both the solvation and rotational dynamics measurements were performed with the fluorescence upconversion technique. To carry out the solvation dynamics experiments, time-resolved fluorescence was detected at different wavelengths with a magic angle polarization configuration for the excitation and the gate pulse in order to cancel out the reorientation contribution of the chromophore. The reorientational dynamics of the chromophore was investigated by measuring the fluorescence depolarization decay of the chromophore at parallel and perpendicular polarization configurations.

The experimental setup for the time-resolved fluorescence upconversion[17,97−99] measurements is depicted in Figure 3. A Ti:sapphire laser (Spectra Physics, Tsunami) was CW pumped by a Nd:YVO_4 laser and provided 80-fs pulses with about 15 nJ of energy per pulse at a repetition rate of 82 MHz. These pulses were frequency doubled to obtain <120-fs laser pulses at a wavelength of 420 nm with about 2 nJ of energy per pulse. The remaining portion of the fundamental laser pulse at 840 nm was separated from the frequency-doubled light and contains an energy of about 8 nJ per pulse.

The frequency-doubled pulse was focused by the lens L1 (50-mm focal length) into the sample. The induced fluorescence was collected by a reflecting microscope objective (Coherent) and collimated by a second lens L2 (50-mm focal length). To adjust the intensity of the excitation laser pulse, an attenuator consisting of a combination of a half wave plate (HW) and a polarizer (Pol) was employed. An additional half-wave plate was used to tune the direction of the polarization of the excitation pulse. The remainder of the fundamental laser pulse at 840 nm was utilized as the gate pulse. To this end, the 840-nm laser pulse could be temporally delayed up to 1 ns with respect to the excitation pulse by means of an optical delay line. This optical delay line was driven by a servo motor system (Newport) with 0.1-μm resolution. The gate pulse and the

fluorescence were superimposed and combined by a polarization-selective beam splitter. In this manner, both pulses were collinearly focused by L3 (25-mm focal length) into the nonlinear optical crystal to achieve highly efficient sum frequency generation. The fluorescence upconverted signal was collimated and focused via L4 and *L5* (both with a 50-mm focal length) in a motor-driven double monochromator (Jobin Yvon H10-D) with 1-nm resolution. The signal at the selected wavelength was then detected by a side-on photomultiplier (PMT) (Hamamatsu R4632). Lock-in detection was applied to reduce the influence of the disturbing background and scattered light on the signal. To this end, the excitation beam was chopped at 400 Hz, and the signal from the photomultiplier was sent to a lock-in amplifier (EG&G 5209) connected to a personal computer. To achieve a satisfying signal-to-noise ratio, the measured signal was averaged by collecting several scans through repeatedly running the delay line. To prevent decomposition of the sample through continuous excitation of a small spot, the sample was mounted on a speaker driven by a 40-Hz source. The speaker itself was attached to a stepper motor moving the sample perpendicular to the direction of the excitation beam.

A suitable Labview (National Instruments) computer program controlling data recording and analysis provides the ability to run the delay line in different intervals with suitable speeds and step sizes. Finally, every scan was saved to eliminate clearly disturbed scans from the ultimate average.

D. Time-Correlated Single-Photon Counting. Since the delay line of the fluorescence upconversion setup is not sufficiently long for measuring the lifetime of C153 in ethanol amounting to about 5 ns, the lifetime of the dye in the samples was determined by a time-correlated single-photon counting (TCSPC) setup. The homebuilt setup of this experiment with excitation pulses centered at 420 nm and with an instrumental response function of about 100 ps (fwhm) is described in detail elsewhere.[100]

E. Data Analysis. The rotational dynamics of the chromophore in bulk ethanol as well as in confined solution was measured by recording the decay of the fluorescence at the wavelength of the fluorescence maximum and with wide monochromator slits (1.5 mm instead of 0.5 mm) to obtain a stronger signal. The fluorescence depolarization was detected at parallel $I_{||}(t)$ and perpendicular $I_{\perp}(t)$ polarization configurations for the excitation and gate beams. Using the fluorescence decays $I_{||}(t)$ and $I_{\perp}(t)$, the time-resolved fluorescence anisotropies[101−103] were calculated by employing eq 1:

$$r(t) = \frac{I_{||}(t) - I_{\perp}(t)}{I_{||}(t) + 2I_{\perp}(t)} \tag{1}$$

This kind of data analysis is valid only if the anisotropy decays to zero for $t = \infty$ As will be seen later in the discussion, the C153 molecules are able to rotate freely in the inner pore volume, and the excitation anisotropy disappears completely by reorientation. The fluorescence depolarization decays $I_{||}(t)$ and $I_{\perp}(t)$ were used without deconvolution since the time scale of the rotational dynamics of C153 is significantly longer than the system response function in all samples investigated.

To elucidate the solvation dynamics of C153 in bulk ethanol as well as in confined solution, the spectral reconstruction method was used to determine the time correlation functions $S(t)$.[17,99] To this end, the time-dependent Stokes shift was measured by utilizing the fluorescence upconversion technique. The fluorescence decay of the chromophore was recorded at 20 different wavelengths in the range from 465 to 600 nm. These data were fit to multiexponential functions using the analysis software RFGraph[104] employing an iterative reconvolution algorithm. A Gaussian fit to the cross-correlation signal of the excitation and the gate pulse with a temporal width of 400 fs (fwhm) was used as a system response function. During this fitting procedure, all parameters were allowed to vary freely with the exception of the slowest decay-time constant attributed to the fluorescence lifetime. These lifetimes were measured independently with the TCSPC setup and were inserted into the fitting function. With the function parameters obtained for each wavelength, simulation graphs $I(t, \lambda_i)$ were calculated for extended time scales (up to 10 ns). These decay curves were normalized through division by the respective integrated decay curve and multiplied by the relative intensity of the emission at the corresponding wavelength in the steady-state fluorescence spectrum $I_{ss}(\lambda_i)$:

$$F(t, \lambda_i) = \frac{I(t, \lambda_i) \times I_{ss}(\lambda_i)}{\int_0^\infty I(\tau, \lambda_i)\, d\tau} \tag{2}$$

After this normalization, the time-resolved fluorescence spectra were reconstructed by plotting $F(t, \tilde{\nu}_i)$ as a function of $\tilde{\nu}_i$, with $\tilde{\nu}_i = 1/\lambda_i$, for different times t. The spectra were reconstructed at 80 distinct times after $t = 0$ in increasing time intervals within the range (0, 3 ns). Reasonably good fits of those spectra were achieved with a log-normal function, as given in eq 3, for all of the measured samples:

$$g(\tilde{\nu}) = h\begin{cases}\exp[-\ln(2)\{(\ln(1+\alpha)/\gamma\}^2] & \alpha > -1 \\ 0 & \alpha \le -1\end{cases}$$
$$\alpha \equiv [2\gamma(\tilde{\nu} - \tilde{\nu}_{max})]/\Delta \tag{3}$$

In this equation, $\tilde{\nu}_{max}$ represents the maximum; Δ, the width; γ, the asymmetry; and h, the amplitude of the spectra. With the peak values $\tilde{\nu}_{max}(t)$ obtained this way, the time correlation function $S(t)$

$$S(t) = \frac{\tilde{\nu}_{max}(t) - \tilde{\nu}_{max}(\infty)}{\tilde{\nu}_{max}(0) - \tilde{\nu}_{max}(\infty)} \tag{4}$$

was calculated. In eq 4, $\tilde{\nu}_{max}(\infty)$ and $\tilde{\nu}_{max}(0)$ are the extrapolated asymptotic values for $\tilde{\nu}_{max}(t)$ for $t = \infty$ and 0, respectively. The time correlation functions computed in this manner were then fit to a triple-exponential function providing the characteristic solvation dynamics decay times and the relative amplitudes of the contributing processes. Additionally the averaged solvation time constants $t_{1/e}$, $\langle\tau\rangle$, and τ^{-1} were calculated. Here, $t_{1/e}$ represents a mean solvation time (the time at which $S(t)$ decreases by a factor of $^1/_e$ with respect to its initial value), whereas $\langle\tau\rangle$ and τ^{-1} emphasize the long- and short-time behavior of the solvation dynamics, respectively.

3. Results and Discussion

A. Absorption and Fluorescence. The absorption and fluorescence spectra of C153 in bulk ethanol and dissolved in ethanol confined in the porous sol−gel samples are shown in Figure 4. In the bottom part of the Figure, the area indicated in the top part is magnified to clarify the changes in the spectra by the influence of the restricted environment. The spectra are all shifted upon inclusion of the solution into the porous sol−gel glass. The measured spectral maxima are collected in Table 1 together with the calculated Stokes shifts. What can be seen

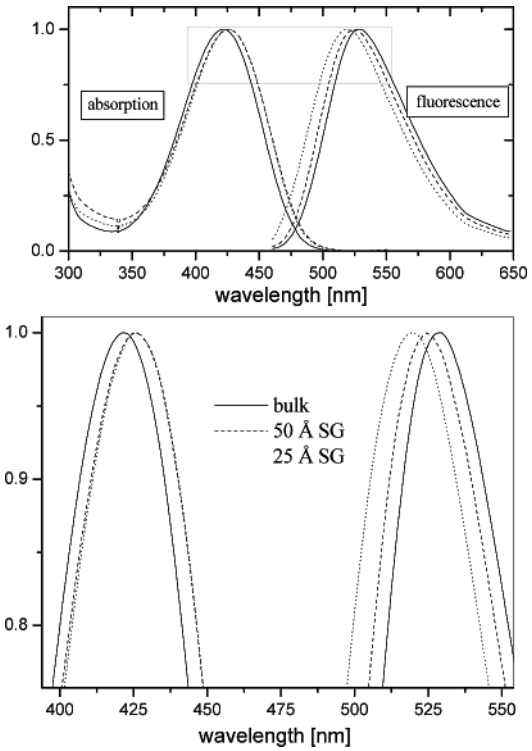

Figure 4. Absorption and fluorescence spectra of C153 in bulk ethanol (—) and solvated in the inner ethanol pools of the sol−gel samples with pore diameters of 50 (- - -) and 25 Å (···).

TABLE 1: Maxima of the Absorption and Emission Spectra of C153 in Confined Ethanol Together with the Calculated Stokes Shift

	bulk	50-Å SG	25-Å SG
absorption λ_{abs} (nm)	421	426	426
fluorescence λ_{flu} (nm)	528	524	519
Stokes shift	107	98	93

from Figure 1 and in Table 1 is a red shift of the absorption spectrum of C153 in confined ethanol. It seems that this absorption shift is independent of the pore size. In contrast, the fluorescence spectra are blue shifted with decreasing pore diameter. Horng et al.[71] as well as Moog et al.[105] investigated the absorption and fluorescence of C153 as a function of solvent polarity. They found that with increasing solvent polarity both the absorption and the emission spectrum of C153 shift to higher wavelengths; furthermore, the overall Stokes shift increases with increasing solvent polarity. According to these studies, the behavior of the absorption spectra presented in our work should be explained in terms of increasing polarity of the solute's environment inside the porous material. The inclusion isotherms in Figure 2 support this explanation as they indicate that C153 is more "soluble" (i.e., its concentration is higher) in the confined ethanol compared to its behavior in the bulk liquid. As will be seen in the discussion of the rotational dynamics data, the chromophore is completely solvated in the spatially confined ethanol within the porous samples, and no adsorption at the pore surface takes place.

However, the fluorescence spectra show the opposite behavior: they move to shorter wavelengths with decreasing pore size. Also, the overall Stokes shift decreases with decreasing pore size. These experimental findings can be explained if one considers that the confinement can induce two effects: the motion of the solvent molecules near the surface can be hindered by the pore walls, and the number of solvent molecules affecting the solute can be smaller than in the bulk (restricted solvation shell). If this is the case, the confinement will prevent the complete solvation of the chromophore (i.e., the distance between the minima of the potential energy surfaces for the ground and the excited state with respect to the solvation coordinate will be reduced). This change will give rise to a red shift of the absorption maximum and a blue shift of the fluorescence peak. A decrease of the overall Stokes shift can be also interpreted in the same way.

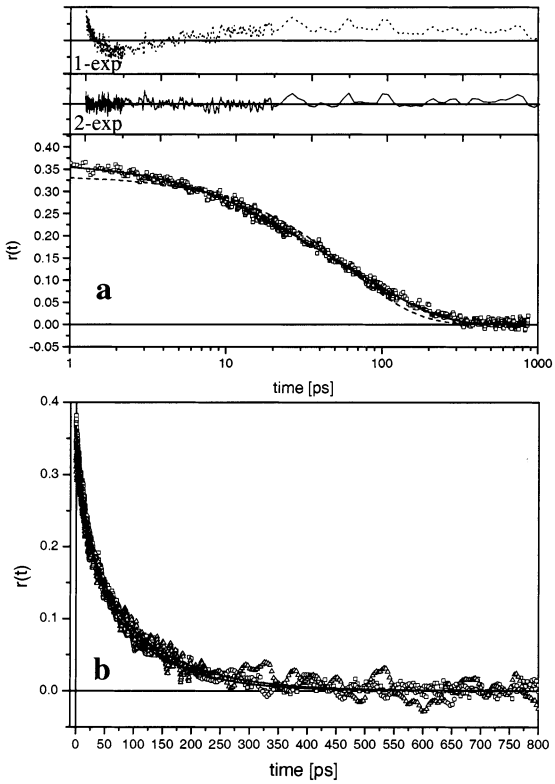

Figure 5. Time-resolved fluorescence anisotropy of (a) C153 in bulk ethanol. The solid curve through the measured data (□) corresponds to a biexponential fitting of the anisotropy data. The dashed line shows the best fit through the data with a single-exponential function. At the top of graph a, the residuals obtained from the single- and double-exponential fits are shown. (b) C153 in bulk ethanol (□) and confined in 50- (○) and 25-Å (△) porous sol−gel glasses.

It should be mentioned, finally, that the decrease of the overall Stokes shift can also be interpreted as a decrease of the dielectric constant of the solvent upon confinement. Such behavior has been observed in numerical simulations of a polar solvent confined in a spherical cavity.[89] The authors attribute the decrease in the dielectric constant to a preferential alignment of the solvent molecules along the pore walls with their dipoles placed in an antiparallel fashion.

B. Anisotropy and Life Time. The time-resolved orientational anisotropy of excited C153 molecules in bulk ethanol is shown in Figure 5 a and b. The measured anisotropy data were first fitted by a single-exponential function yielding the dashed curve and providing the residuals presented in Figure 5a. Obviously, one exponential function does not satisfactorily describe the measured anisotropy decay. This observation was also found for C153 in various solvents by Maroncelli et al.[17] and Horng et al.[93] These authors associated this nonexponential behavior with a departure of the rotational motion from the strict Markovian limit (i.e., slow time-dependent friction components influence the rotational motion of the chromophore). Via model calculations, Horng et al.[93] found a direct correspondence between those polar solvents showing clear nonexponential anisotropy behavior and those whose solvation correlation

TABLE 2: Time-Resolved Anisotropy Parameters and Fluorescence Lifetimes of C153 in Bulk Ethanol and Confined in 50- and 25-Å Sol−Gel Glasses

	bulk	50-Å SG	25-Å SG
anisotropy r_0	0.366 ± .005	0.368 ± 0.005	0.337 ± 0.005
τ_{rot1} (ps)	14 ± 1	18 ± 1	17 ± 1
τ_{rot2} (ps)	92 ± 2	97 ± 4	110 ± 4
$\langle\tau_{rot}\rangle$ (ps)	67 ± 1	64 ± 4	75 ± 4
τ_L (ps)	4850	4910	5060

functions comprise significant components decaying with time constants greater than one-fifth of the observed solute mean rotational time. They proposed the utilization of an average anisotropy decay time defined as

$$\langle\tau_{rot}\rangle = a\tau_1 + (1 - a)\tau_2 \quad (5)$$

to compare the rotational diffusion times measured within different environments as well as the one obtained with theoretical models. For an extensive theoretical description of the rotational motion of C153 in a large variety of solvents in terms of hydrodynamic models including dielectric friction, we therefore refer to this article.

The experimental data obtained from our measurements are summarized in Table 2. The anisotropy decay parameters in bulk ethanol are very close to the results published by Horng et al.[93] ($r_0 = 0.375$, $a = 0.337$, $\tau_1 = 10.4$ ps, $\tau_2 = 89$ ps, $\langle\tau_{rot}\rangle = 63$ ps).

By comparing the anisotropy decay data in bulk ethanol and the results in confined ethanol, the following observations can be made: The value of the initial anisotropy $r_0 = r(t = 0)$ does not change considerably when the ethanol solution is confined to the porous sol−gel glasses. This indicates that C153 can rotate freely even inside the porous matrix. The slight decrease of r_0 in the 25-Å sol−gel glass is not substantial (<10%) so that we rather ascribe it to the poorer signal-to-noise ratio than to an indication of adsorbed dye molecules. This is in contrast to an earlier investigation by us[90] of the molecular dynamics of the ionic chromophore nile blue in the same porous systems, where a majority of chromophores were adsorbed at the inner pore surfaces. The same is true for most publications concerning dye solutions in contact with glassy or crystalline surfaces[106−111] where (even if not explicitly emphasized) an immobile phase of chromophores is observed. In the case here, however, because of the weak interaction between chromophore and modified surface, the C153 molecules are completely solvated in the inner pore volume.

The biexponential character of the anisotropy decay is also found in the confined ethanol samples. Regarding the mean rotational decay times $\langle\tau_{rot}\rangle$, the chromophore in the 50-Å sol−gel behaves as it does in the bulk, whereas in the 25-Å pores the rotation is slightly retarded. Because the chromophores are not adsorbed, the slowing down of the rotational diffusion in the smaller pores must be an effect of restricted geometry. This behavior can be explained by considering that the rotational dynamics of the chromophore is strongly affected by the viscosity of the solvent. Previous studies of reorientational dynamics show that indeed liquids confined inside a restricted geometry are characterized by a solvent layer near the surface whose viscosity is higher than that of the inner solvent, which is bulklike. In the following discussion, these studies are recalled in some details.

Awschalom and co-workers were the first to study reorientational dynamics of liquids in restricted geometries.[43−45] They investigated CS_2 and nitrobenzene in the 22-Å-radius pores of a sol−gel glass with an OKE setup.[43] Whereas in bulk nitrobenzene the rotational diffusion is characterized by a single time constant of 39 ps, the experimental signal of confined nitrobenzene exhibits a biexponential decay with a second time constant of 126 ps. The authors attribute this second contribution to nitrobenzene molecules in a more viscous surface layer. In contrast to this, they do not observe any difference between bulk and confined CS_2 and cannot find evidence for a more viscous surface layer in this liquid with weak surface interaction.

In a variety of publications about NMR investigations on the dynamics of confined liquids ranging from acetonitrile to aniline and cyclohexane, Jonas et al.[33,35,61−64,112−114] observed an interfacial solvent layer with properties such as viscosity and density differing from those of the bulk. A second liquid phase in the inner volume of the pores, however, has bulklike behavior. This "two-state fast exchange model" was further used by Fourkas et al.[38−40] to explain rotational diffusion times of confined liquids measured with OKE spectroscopy. They also found a bulklike phase and a more viscous surface layer for CS_2,[38] acetonitrile,[39] and methyliodide[40] and evaluate the exchange between these two layers.

If one considers that on average the solute molecule is set at the center of the pore, then the onset of the slowing down of the rotational motions at a distinct pore size leads to the conclusion that the characteristic correlation length for rotational motion in the case considered here is in the range of 15−25 Å.

However, it is not possible to exclude the fact that some of the C153 chromophores reside near the pore surface. The existence of an interfacial solvent layer with increased viscosity is likely to cause retardation in the rotational dynamics of these chromophores. This situation will be more likely the smaller the pore size. In such a case, the viscosity of the liquid surrounding the solute near the pore wall will be greater than the one experienced by solute molecules placed far from it. The decay time of the anisotropy $r(t)$ should show a decrease caused by the different surroundings that the chromophores can experience in going from the center of the pore toward the pore walls. Our experimental findings support such a picture only for the sample with the 25-Å pores.

In Table 2, the measured lifetimes of C153 in the confined liquid are presented, too. There is a small increase in the fluorescence lifetime with decreasing pore size. However, the effect is small (<5%) compared to the increase in the lifetime observed for nile blue in the same porous system (>85%).[90] An increased lifetime in confined liquid solution has also been measured by other authors.[54−56,116] These groups ascribe the lifetime effect to reduced polarity through a decreased number of solvent molecules inside the cage structure. A similar effect in solvents of various polarity was observed with coumarin 153 by Maroncelli et al.[17] The reduced polarity of the surrounding solvent might block some internal relaxation channels and in this way slow the ground-state recovery.

C. Solvation Dynamics. To compare the extent of solvation of C153 in the confined solutions with that in bulk ethanol, the time-dependent peak-shift value $\nu(t) - \nu(\infty)$ obtained from log-normal fits to each of the reconstructed spectra have been depicted for all three samples in Figure 6.

The amplitude of the dynamic Stokes shift ($\nu(0) - \nu(\infty)$) for C153 in bulk ethanol found here is much smaller than the one measured by Horng et al.[71] Those authors observed for the same system a Stokes shift of about 2000 cm^{-1}, which is about twice the value we found. We associate this discrepancy with the superior time resolution of that group in contrast to our system response of about 400 fs. As a result, we have not been able to

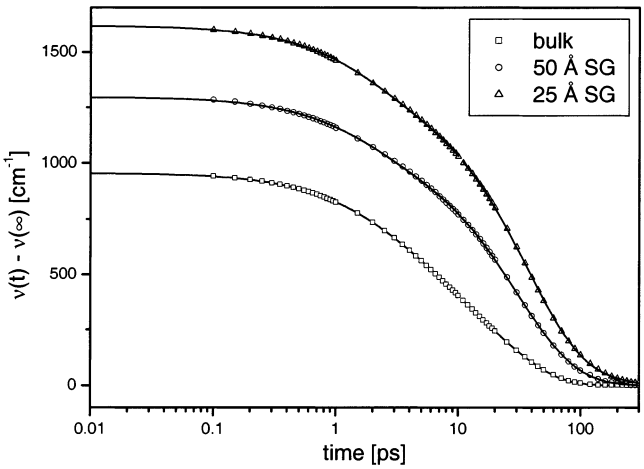

Figure 6. Dynamic shift of peak values $\nu(t) - \nu(\infty)$ of the log-normal fits to the reconstructed spectra for C153 in bulk ethanol (□) and confined in 50- (○) and 25-Å (△) sol−gel glasses.

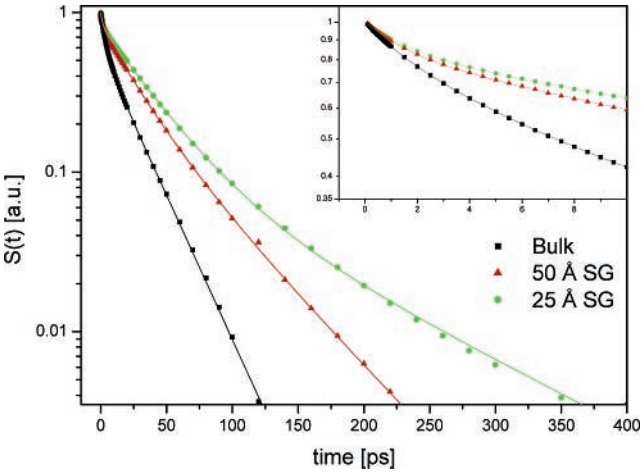

Figure 7. Time correlation function of the solvation dynamics of C153 in bulk ethanol (■) and confined in 50- (●) and 25-Å (▲) sol−gel glasses.

detect the ultrafast dynamics that can be responsible for a considerable part of the solvation.

The dynamic Stokes shift observed in the confined solutions increases with decreasing pore diameter. Since the overall Stokes shift ($\nu_{abs} - \nu_{flu}$) diminishes with decreasing pore size, the only realistic explanation for this behavior is a slowing down of the solvent reorganization as a result of confinement. In this case, the contributions of ultrafast dynamics decrease in favor of slower solvation processes detectable in the time window of our experiment.

Normalizing the time-dependent Stokes shift ($\nu(t) - \nu(\infty)$) by the total dynamic shift ($\nu(0) - \nu(\infty)$) leads to the time correlation functions $S(t)$ shown in Figure 7 for the different samples. The fit parameters for the $S(t)$ functions are summarized in Table 3. Besides the absence of ultrafast components, the agreement of the decay time constants observed for C153 in bulk ethanol with the results of Horng et al.[71] is quite good. An extensive experimental and theoretical description of the solvation dynamics of C153 in several solvents has already been published by other groups,[18,71,72,91,92,116,117] and we refer to those publications for theoretical aspects.

By comparing the $S(t)$ curves of C153 in bulk solution with that in confined systems, we see that a continuous slowing down of the solvation dynamics emerges. It affects not only the overall solvation process, which is well represented by the global decay

TABLE 3: Fit Parameters of the Correlation Functions $S(t)$ for C153 in Ethanol and Confined in 50- and 25-Å Pores

	bulk	50-Å SG	25-Å SG
a_1	0.17	0.18	0.17
τ_1 (ps)	1.5	1.7	1.8
a_2	0.34	0.51	0.70
τ_2 (ps)	6.6	24.3	34.0
a_3	0.50	0.31	0.12
τ_3 (ps)	26.3	50.7	102.7
$t_{1/e}$ (ps)	12.5	25.5	32.0
τ^0 (ps)	5.4	7.6	8.4
$\langle\tau\rangle$ (ps)	15.5	28.6	36.9

time constants $t_{1/e}$ and $\langle\tau\rangle$, but also has an impact on every individual solvation time τ_i. And although the relative amplitude of the fastest process is unchanged upon confinement, the amplitude of the slowest dynamics decreases in favor of the intermediate process with decreasing pore size.

Because polar solvation dynamics is first of all controlled by electrostatic interactions between the solute dipole and the dipoles of the solvent molecules, the modified polarization field is likely to be the origin of the slowing down of the solvation dynamics with decreasing pore size. As mentioned previously, inside the cavity there is a preferential alignment of the solvent molecules resulting in an effective lowering of the dielectric constant compared to that of the bulk system. According to continuum theories of solvation,[16,74,118−120] the decay times τ_i of solvation dynamics are inversely proportional to the corresponding dielectric constant ϵ_i. Therefore, on the basis of the modified polarization-field model, a slowing down of the solvation process can be expected in confined solutions.

Of course, the interfacial solvent layer may also participate in the retardation of solvation, especially in smaller pores. If the pore size is small enough for the solvent molecules in the highly viscous surface layer to contribute to the stabilization of the system energy, then the dielectric constant is further diminished by the prealignment of the solvent molecules along the pore surface.

It is difficult to quantify the contributions of both effects to the slowing down of the solvation dynamics. Since they are both qualitative models and the influence of additional effects cannot be excluded, we restrict ourselves to this simple description of the observed phenomena. We hope, however, that the results presented here can form the basis for theoretical model calculations and simulations of confined solutions.

Time-resolved anisotropy and solvation dynamics measurements at room temperature were also published by several other groups. Levinger and co-workers[57−59,65,121] presented a variety of studies about the solvation dynamics of coumarin 343 (C343) solutions confined in AOT reverse micelles with an inner cage diameter of 30 to 200 Å. Their investigations on C343/water/AOT/isooctane revealed a significant slowing down of the solvation dynamics with decreasing micelle size. The Stokes shift measured in those investigations diminished with decreasing micelle diameter. Even in the largest micelles, no bulk behavior of the solvation dynamics in the inner water pools could be found. In the smallest micelles, a complete freezing of the water associated with a total disappearance of solvation dynamics was observed.[57] This immobilization was also found for confined formamide.[59] By changing the ion at the hydrophilic group of the micelle,[65,121] this group ascertained that the interaction of surfactant water molecules inside the micelle with the specific ion at the inner micellar group is important. Nevertheless, according to Riter et al.,[57] the influence of this counterion does not account for the whole difference of the

solvation dynamics in bulk water and in the inner micellar water pools. Additional confinement effects play a role in retarding the solvation dynamics.

Another interesting result was found by Shirota and Horie[122] while investigating C343/methol/AOT/heptane and C343/acetonitrile/AOT/heptane with a time resolution of about 50 ps. Whereas the solvation dynamics of C343 in confined methanol showed a clear dependence on the size of the micelle, the solvation dynamics of C343 in acetonitrile was independent of the diameter of the inner liquid pool. The authors argued that this behavior is due to the intermolecular network of H bonds in methanol, which transfers the strong interfacial interactions between the surface and solvent to the inner volume of the liquid pool inside the micelle. Because of their relatively poor time resolution, they were not able to obtain information about faster relaxation processes in their confined solutions.

As mentioned in the Introduction, other investigations[48,54−56] of liquids in micellar environments have also seen a clear slowing down of the dynamics observed. Similar results were obtained from measurements in cyclodextrines[53] and vesicles.[123]

4. Conclusions

In this paper, we have presented measurements of solvation dynamics and time-resolved anisotropy in a room-temperature liquid confined to a mesoporous sol−gel host. These experiments have allowed us to gain information about the influence of geometrical restrictions and surface interactions on the characteristics of dynamics in this liquid.

In particular, we have investigated the static and dynamic fluorescence properties as well as the fluorescence anisotropy of a coumarin 153/ethanol solution confined in sol−gel glasses with 50- and 25-Å average pore sizes and have compared them with the bulk behavior.

Both the amplitude of the dynamic Stokes shift and the time behavior of the solvation process are drastically changed. Whereas the static Stokes shift decreases with decreasing pore size, the measured dynamic Stokes shift shows the opposite behavior. This effect can be explained by a decreasing amplitude of ultrafast events in favor of slower solvation processes.

The solvation dynamics in the confined solution show nonexponential behavior comparable to that of the bulk. All contributions to the solvation process slow down, and the individual decay time constants characterizing it increase with the decreasing pore size of the sol−gel glass. Two phenomenological models have been put forward to explain these effects. The modified polarization field model takes into account the confinement and predicts a strengthening of the solvent's reaction field induced by a preferential alignment of the solvent molecules inside the pore. The model of the surface solvent layer focuses on the interactions of the solvent molecules with the inner pore surface and assumes a higher viscosity for this superficial solvent layer, resulting in longer relaxation times. Probably both effects are of relevance in the confined solutions investigated.

Regarding the time-resolved anisotropy of the C153 chromophore in confined solution, no significant change has been observed for both the inertial anisotropy r_0 and the mean rotational diffusion time $\langle\tau_{rot}\rangle$ upon confining the bulk solution in the sol−gel glass with a 50-Å pore diameter. In contrast, a nonnegligible slowing down of the rotational diffusion is seen for the solution confined in 25-Å pore samples.

The solvation dynamics measurements presented here allow no determination of a particular correlation length. It seems that the confinement strongly affects the behavior of the solvent molecules surrounding the solute and affecting its solvation. Upon comparing these solvation results with the data for nile blue in confined ethanol, no significant difference is seen.

To test the universality of the results presented here, further experiments are necessary. In particular, the influence of different solvent polarity and proticity has to be clarified. In addition, theoretical calculations and computer simulations are needed to understand the effects observed in this publication more thoroughly.

Acknowledgment. We thank the Deutsche Forschungsgemeinschaft (DFG) for their support of this work under grant De446/2-2.

References and Notes

(1) Born, M. *Z. Phys.* **1920**, *1*, 1.
(2) Onsager, L. *J. Am. Chem. Soc*. **1936**, *58*, 1486.
(3) Debye, P. *Polar Molecules*; Dover: New York, 1929.
(4) Einstein, A. *Ann. Phys*. **1906**, *19*, 371.
(5) Stokes, G. *Trans. Cambridge Philos. Soc*. **1856**, *9*, 5.
(6) Perrin, F. *J. Phys. Radium* **1934**, *5*, 497.
(7) Garg, S. K.; Smyth, C. P. *J. Phys. Chem*. **1965**, *69*, 129.
(8) Barthel, J.; Bachhuber, K.; Buchner, R.; Hetzenauer, H. *Chem. Phys. Lett*. **1990**, *165*, 369.
(9) Kindt, J. T.; Schmuttenmaer, C. A. *J. Phys. Chem.* **1996**, *100*, 10373.
(10) Lippert, E. *Z. Naturforsch. A: Phys. Sci.* **1955**, *10*, 541.
(11) Mataga, N. *Bull. Chem. Soc. Jpn.* **1963**, *36*, 654.
(12) Marcus, R. A. *J. Chem. Phys*. **1963**, *39*, 1734.
(13) Ooshika, Y. *J. Phys. Soc. Jpn.* **1954**, *9*, 594.
(14) Onsager, L. *Can. J. Chem*. **1977**, *55*, 1819.
(15) Wolynes, P. G. *Annu. Rev. Phys. Chem*. **1980**, *31*, 345.
(16) van der Zwan, G.; Hynes, J. T. *J. Phys. Chem*. **1985**, *89*, 4181.
(17) Maroncelli, M.; Fleming, G. R. *J. Chem. Phys*. **1987**, *86*, 6221.
(18) Maroncelli, M. *J. Chem. Phys.* **1997**, *106*, 1545.
(19) Raineri, F. O.; Friedman, H. L.; Perng, B.-C. *J. Mol. Liq.* **1997**, *73*, 419.
(20) Polimeno, A.; Saielli, G.; Nordio, P. L. *Chem. Phys.* **1998**, *235*, 313.
(21) Roy, S.; Bagchi, B. *J. Chem. Phys.* **1994**, *101*, 4150.
(22) Rips, I.; Klafter, J.; Jortner, J. *J. Chem. Phys.* **1988**, *88*, 3246.
(23) Rosenthal, S. J.; Jimenez, R.; Fleming, G. R.; Kumar, P. V.; Maroncelli, M. *J. Mol. Liq.* **1994**, *60*, 25.
(24) Stratt, R. M.;.Maroncelli, M. *J. Phys. Chem*. **1996**, *100*, 12981.
(25) Bagchi, B. *J. Chem. Phys.* **1994**, *100*, 6658.
(26) Cho, M.; Rosenthal, S. J.; Scherer, N. F.; Ziegler, L. D.; Fleming, G. R. *J. Chem. Phys.* **1992**, *96*, 5033.
(27) Ladanyi, B. M.; Maroncelli, M. *J. Chem. Phys*. **1998**, *109*, 3204.
(28) Barbara, P. F.; Jarzeba, W. *Adv. Photochem*. **1990**, *15*, 1.
(29) Klafter, J.; Drake, J. M. *Molecular Dynamics in Restricted Geometries*; Wiley: New York, 1989.
(30) Drake, J. M.; Klafter, J. *Phys. Today* **1990**, 46.
(31) *Dynamics in Small Confining Systems*; Materials Research Society Symposium Proceedings, Boston, MA, November 30−December 4, 1992; Drake, J. M., Klafter, J., Kopelman, R. R., Awschalom, D. D., Eds.; Materials Research Society: Pittsburgh, PA, 1993.
(32) *Dynamics in Small Confining Systems*; Materials Research Society Symposium Proceedings, Boston, MA, November 28−December 1, 1994; Drake, J. M., Troian, S. M., Klafter, J., Kopelman, R., Eds.; Materials Research Society: Pittsburgh, PA, 1995.
(33) Liu, G.; Mackowiak, M.; Li, Y.; Jonas, J. *J. Chem. Phys.* **1991**, *94*, 239.
(34) Wallen, S. L.; Nikiel, L.; Jonas, J. *J. Phys. Chem.* **1995**, *99*, 15421.
(35) Korb, J. P.; Malier, L.; Cros, F.; Xu, S.; Jonas, J. In *Dynamics in Small Confining Systems*; Materials Research Society Symposium Proceedings, Boston, MA, December 2−4, 1996; Drake, J. M., Klafter, J., Kopelman, R. R., Eds.; Materials Research Society: Pittsburgh, PA, 1997; p 9.
(36) Schwalb, G.; Deeg, F. W. *Phys. Rev. Lett*. **1995**, *74*, 1383.
(37) Carini, G.; Crupi, V.; D'Angelo, G.; Majolino, D.; Migliardo, P.; Mel'nichenko, Y. B. J. *Chem. Phys*. **1997**, *107*, 2292.
(38) Farrer, R. A.; Loughnane, B. J.; Fourkas, J. T. *J. Phys. Chem. A* **1997**, *101*, 4005.
(39) Loughnane, B. J.; Farrer, R. A.; Fourkas, J. T. *J. Phys. Chem. B* **1998**, *102*, 5409.
(40) Loughnane, B. J.; Fourkas, J. T. *J. Phys. Chem.* **1999**, *102*, 10288.
(41) L'Espérance, D.; Chronister, E. L. *Chem. Phys. Lett.* **1993**, *201*, 229.

(42) Nikiel, L.; Hopkins, B.; Zerda, T. W. *J. Phys. Chem.* **1990**, *94*, 7458.
(43) Warnock, J.; Awschalom, D. D.; Shafer, M. W. *Phys. Rev. B* **1986**, *34*, 475.
(44) Warnock, J.; Awschalom, D. D.; Shafer, M. W. *Phys. Rev. Lett.* **1986**, *57*, 1753.
(45) Warnock, J.; Awschalom, D. D. *Phys. Rev. B* **1987**, *35*, 1962.
(46) Schwarz, V.; Deeg, F. W.; Bräuchle, C. To be submitted for publication.
(47) Schwalb, G.; Deeg, F. W.; Bräuchle, C. *J. Non-Cryst. Solids* **1994**, *172*−*174*, 348.
(48) Lundgren, J. S.; Heitz, M. P.; Bright, F. V. *Anal. Chem.* **1995**, *67*, 3775.
(49) Streck, C.; Melnichenko, Y. B.; Richert, R. *Phys. Rev. B* **1996**, *53*, 5341.
(50) Yan, X.; Streck, C.; Richert, R. Discussion Meeting of the Deutsche Bunsen-Gesellschaft für Physikalische Chemie Physical Chemistry of Glasses, Jena, Germany, 1996.
(51) Richert, R. *Phys. Rev. B* **1996**, *54*, 15762.
(52) Das, K.; Sarkar, N.; Das, S.; Datta, A.; Bhattacharyya, K. *Chem. Phys. Lett*. **1996**, *249*, 323.
(53) Vajda, S.; Jiminez, R.; Rosenthal, S. J.; Fidler, V.; Fleming, G. R.; Castner, E. W. *J. Chem. Soc., Faraday Trans.* **1995**, *91*, 867.
(54) Datta, A.; Mandal, D.; Pal, S. K.; Bhattacharyya, K. *J. Phys. Chem. B* **1997**, *101*, 10221.
(55) Datta, A.; Mandal, D.; Pal, S. K.; Bhattacharyya, K. *Chem. Phys. Lett.* **1997**, *228*, 77.
(56) Das, S.; Datta, A.; Bhattacharyya, K. *J. Phys. Chem. A* **1997**, *101*, 3299.
(57) Riter, R. E.; Willard, D. M.; Levinger, N. E. *J. Phys. Chem. B* **1998**, *102*, 2705.
(58) Willard, D. M.; Riter, R. E.; Levinger, N. E. *J. Am. Chem. Soc.* **1998**, *120*, 4151.
(59) Riter, R. E.; Undiks, E. P.; Kimmel, J. R.; Levinger, N. E. *J. Phys. Chem. B* **1998**, *102*, 7931.
(60) Yanagimachi, M.; Tamai, N.; Masuhara, H. *Chem. Phys. Lett.* **1992**, *200*, 469.
(61) Liu, G.; Li, Y.; Jonas, J. *J. Chem. Phys.* **1991**, *95*, 6892.
(62) Korb, J. P.; Delville, A.; Shu, X.; Demeulenaere, G.; Costa, P.; Jonas, J. *J. Chem. Phys.* **1994**, *101*, 7074.
(63) Korb, J.-P.; Malier, L.; Cros, F.; Xu, S.; Jonas, J. *Phys. Rev. Lett.* **1996**, *77*, 2312.
(64) Korb, J. P.; Shu, X.; Jonas, J. *J. Chem. Phys.* **1993**, *98*, 2411.
(65) Riter, R. E.; Undinks, E. P.; Levinger, N. E. *J. Am. Chem. Soc.* **1998**, *120*, 6062.
(66) Cho, C. H.; Chung, M.; Lee, J.; Nguyen, T.; Singh, S.; Vedamuthu, M.; Yao, S.; Zhu, J.-B.; Robinson, G. W. *J. Phys. Chem.* **1995**, *99*, 7806.
(67) L'Espérance, D.; Chronister, E. L. *Chem. Phys. Lett.* **1994**, *222*, 217.
(68) Cichos, F.; Willert, A.; Rempel, U.; von Borczyskowski, C. *J. Phys. Chem.* A **1997**, *101*, 8179.
(69) Kahlow, M. A.; Jarzeba, W.; Tai Jong, K.; Barbara, P. F. *J. Chem. Phys.* **1989**, *90*, 151.
(70) Castner, E. W., Jr.; Maroncelli, M.; Fleming, G. R. *J. Chem. Phys.* **1987**, *86*, 1090.
(71) Horng, M. L.; Gardecki, J. A.; Papazyan, A.; Maroncelli, M. *J. Phys. Chem.* **1995**, *99*, 17311.
(72) Reynolds, L.; Gardecki, J. A.; Frankland, S. J. V.; Horng, M. L.; Maroncelli, M. *J. Phys. Chem.* **1996**, *100*, 10337.
(73) Fourkas, J. T.; Berg, M. *J. Chem. Phys.* **1993**, *98*, 7773.
(74) Bagchi, B.; Oxtoby, D. W.; Fleming, G. R. *Chem. Phys*. **1984**, *86*, 257.
(75) Bagchi, B. *Annu. Rev. Phys. Chem.* **1989**, *40*, 115.
(76) Berg, M. *J. Phys. Chem. A* **1998**, *102*, 17.
(77) Maroncelli, M.; Fleming, G. R. *J. Chem. Phys.* **1988**, *89*, 875.
(78) Roy, S.; Bagchi, B. *Proc. Indian Acad. Sci., Chem. Sci.* **1993**, *105*, 295.
(79) Bagchi, B.; Chandra, A. *J. Chem. Phys.* **1992**, *97*, 5126.
(80) Rainieri, F. O.; Resat, H.; Perng, B.-C.; Hirata, F.; Friedman, H. L. *J. Chem. Phys*. **1994**, *100*, 1477.
(81) Bruehl, M.; Hynes, J. T. *J. Phys. Chem.* **1992**, *96*, 4068.
(82) Ladanyi, B. M.; Skaf, M. S. *Annu. Rev. Phys. Chem.* **1993**, *44*, 335.
(83) Schueller, J.; Mel'nichenko, Y. B.; Richert, R.; Fischer, E. W. *Phys. Rev. Lett.* **1994**, *73*, 2224.
(84) Schueller, J.; Richert, R.; Fischer, E. W. *Phys. Rev. B* **1995**, *52*, 15232.
(85) Mel'nichenko, Y. B.; Schueller, J.; Richert, R.; Ewen, B.; Loong, C.-K. *J. Chem. Phys.* **1995**, *103*, 2016.
(86) Nandi, N.; Bagchi, B. *J. Phys. Chem.* **1996**, *100*, 13914.
(87) Nandi, N.Bagchi, B. *J. Phys. Chem. B* **1997**, *101*, 10954.
(88) Senapati, S.; Chandra, A. *Chem. Phys.* **1998**, *231*, 65.
(89) Senapati, S.; Chandra, A. *J. Chem. Phys.* **1999**, *111*, 1223.
(90) Baumann, R.; Ferrante, C.; Deeg, F. W.; Bräuchle, C. *J. Chem. Phys.* **2001**, *114*, 5781.
(91) Gardecki, J.; Horng, M. L.; Papazyan, A.; Maroncelli, M. Yamada 42nd Conference, Nagoya, Japan, 1994.
(92) Gardecki, J. A.; Maroncelli, M. *Chem. Phys. Lett.* **1999**, *301*, 571.
(93) Horng, M. L.; Gardecki, J. A.; Maroncelli, M. *J. Phys. Chem. A* **1997**, *101*, 1030.
(94) Jiang, Y.; McCarthy, P. K.; Blanchard, G. *J. Chem. Phys.* **1994**, *183*, 249.
(95) Kovalenko, S. A.; Ruthmann, J.; Ernsting, N. P. *Chem. Phys. Lett.* **1997**, *271*, 40.
(96) Maroncelli, M.; Fee, R. S.; Chapman, C. F.; Fleming, G. R. *J. Phys. Chem.* **1991**, *95*, 1012.
(97) Hallidy, L. A.; Topp, M. R. *J. Phys. Chem*. **1978**, *82*, 2273.
(98) Lessing, H. E.; Reichert, M. *Chem. Phys. Lett*. **1977**, *46*, 111.
(99) Kahlow, M. A.; Jarzeba, W.; DuBruil, T. P.; Barbara, P. F. *Rev. Sci. Instrum*. **1988**, *59*, 1098.
(100) Rau, J.; Ferrante, C.; Kneuper, E.; Deeg, F. W.; Bräuchle, C. *J. Phys. Chem. B*, submitted for publication.
(101) Fleming, G. R.; Morris, J. M.; Robinson, G. W. *Chem. Phys*. **1976**, *17*, 91.
(102) Tao, T. *Biopolymer*s **1969**, *8*, 609.
(103) Fleming, G. R. *Chemical Applications of Ultrafast Spectroscopy*; Oxford University Press: New York, 1986.
(104) Francis, R. Private communication, 1998.
(105) Moog, R. S.; Davis, W. W.; Ostrowski, S. G.; Wilson, G. L. *Chem. Phys. Lett*. **1999**, *299*, 265.
(106) Anfinrud, P.; Crackel, R. L.; Struve, W. S. *J. Phys. Chem.* **1984**, *88*, 5873.
(107) Anfinrud, P. A.; Causgrove, T. P.; Struve, W. S. *J. Phys. Chem.* **1986**, *90*, 5887.
(108) Crackel, R. L.; Struve, W. S. *Chem. Phys. Lett.* **1985**, *120*, 473.
(109) Meech, S. R.; Yoshihara, K. *Chem. Phys. Lett.* **1989**, *154*, 20.
(110) Morgenthaler, M. J. E.; Meech, S. R. *Chem. Phys. Lett.* **1993**, *202*, 57.
(111) Huston, A. L.; Reimann, C. T. *Chem. Phys.* **1991**, *149*, 401.
(112) Korb, J. P.; Shu, X.; Cros, F.; Malier, L.; Jonas, J. *J. Chem. Phys.* **1997**, *107*, 4044.
(113) Zhang, J.; Jonas, J. *J. Phys. Chem.* **1994**, *98*, 6835.
(114) Sullivan, V. S.; Kim, Y. J.; Xu, S.; Jonas, J.; Korb, J.-B. *Langmuir* **1999**, *15*, 4664.
(115) Balabai, N.; Linton, B.; Napper, A.; Priyadarshy, S.; Sukharevsky, A. P.; Waldeck, D. H. *J. Phys. Chem. B* **1998**, *102*, 9617.
(116) Kovalenko, S. A.; Ruthmann, J.; Ernsting, N. P. *Chem. Phys. Lett.* **1997**, *271*, 40.
(117) Chapman, C. F.; Maroncelli, M. *J. Phys. Chem.* **1991**, *95*, 9095.
(118) Böttcher, C. J. F.; Bordewijk, P. *Theory of Electric Polarization*, 2nd ed.; Elsevier: Amsterdam, 1978.
(119) Castner, E. W.; Fleming, G. R.; Bagchi, B.; Maroncelli, M. *J. Chem. Phys.* **1988**, *89*, 3519.
(120) Castner, E. W.; Bagchi, B.; Maroncelli, M.; Webb, S. P.; Ruggiero, A. J.; Fleming, G. R. *Ber. Bunsen-Ges.* **1988**, *92*, 363.
(121) Pant, D.; Riter, R. E.; Levinger, N. E. *J. Chem. Phys.* **1998**, *109*, 9995.
(122) Shirota, H.; Horie, K. *J. Phys. Chem. B* **1999**, *103*, 1437.
(123) Datta, A.; Pal, S. K.; Mandal, D.; Bhattacharyya, K. *J. Phys. Chem. B* **1998**, *102*, 6114.
(124) Pal, S. K.; Sukul, D.; Mandal, D.; Sen, S.; Bhattacharyya, K. *J. Phys. Chem. B* **2000**, *104*, 2613.